

Noninvasive aortic imaging

Vinit Baliyan, Daniel Verdini, Nandini M. Meyersohn

Division of Cardiovascular Imaging, Department of Radiology, Massachusetts General Hospital, Boston, MA, USA

Contributions: (I) Conception and design: NM Meyersohn; (II) Administrative support: None; (III) Provision of study materials or patients: None; (IV) Collection and assembly of data: None; (V) Data analysis and interpretation: None; (VI) Manuscript writing: All authors; (VII) Final approval of manuscript: All authors.

Correspondence to: Vinit Baliyan, MD. Division of Cardiovascular Imaging, Department of Radiology, Massachusetts General Hospital, Boston, MA, USA. Email: vbaliyan@mgh.harvard.edu.

Abstract: Non-invasive imaging of the aorta has undergone considerable advancements in recent times; largely driven by the technological advances in computed tomography (CT) and magnetic resonance imaging (MRI). This review article highlights these recent advancements and discusses the current role of different imaging tools in the management of aortic diseases.

Keywords: Magnetic resonance imaging (MRI); computed tomography (CT); aortic dissection, aortic aneurysm; aortitis

Submitted Oct 15, 2017. Accepted for publication Dec 04, 2017.

doi: 10.21037/cdt.2018.02.01

View this article at: <http://dx.doi.org/10.21037/cdt.2018.02.01>

Introduction

Imaging plays a crucial role in treatment planning and post-surgical surveillance of aortic pathology. The success of endovascular methods, hybrid approaches, and transcatheter techniques in the treatment of aortic abnormalities has further increased the amount of imaging performed, as these patients require lifelong surveillance. Aortic CT angiography (CTA) with intravenous iodinated contrast material is the most widely used diagnostic modality for a large number of clinical situations. CTA has many advantages including wide availability, rapid acquisition, sub-millimeter spatial resolution and high value in guiding patient management. Disadvantages include the need for iodinated contrast material and ionizing radiation exposure. CT technology has gone through continuous evolution from its inception and recent advances including dual energy capabilities, rapid gantry rotation, fast table movement and high output tubes have allowed for reduction in both iodinated contrast dose and radiation exposure. Advancements in MR technology now also allow scanning without intravenous contrast material as well as more rapid image acquisition than in the past.¹⁸F-fluorodeoxyglucose-

positron emission tomography/computed tomography (¹⁸F-FDG-PET/CT) imaging is useful for the evaluation of vascular graft related infections, large vessel vasculitis and atherosclerotic plaque inflammation. Contrast enhanced ultrasound (CEUS) is also emerging as a method of surveillance for the post-surgical abdominal aorta and has a potential to curb the costs and radiation exposure related to aortic imaging. The purpose of this review is to discuss the use of these noninvasive aortic imaging modalities with a focus on recent advancements.

CTA of the aorta

Indications for aorta CTA

CTA is often the diagnostic modality of choice for the assessment of aortic aneurysms and dissections. Indications for aortic CTA include suspected acute aortic syndromes, aortic aneurysms, post-surgical or endovascular repair imaging surveillance, assessment prior to transcatheter aortic valve replacement (TAVR), monitoring of congenital conditions such as coarctation of the aorta and bicuspid aortic valve with aortopathy, and inflammatory and infectious aortic disorders.

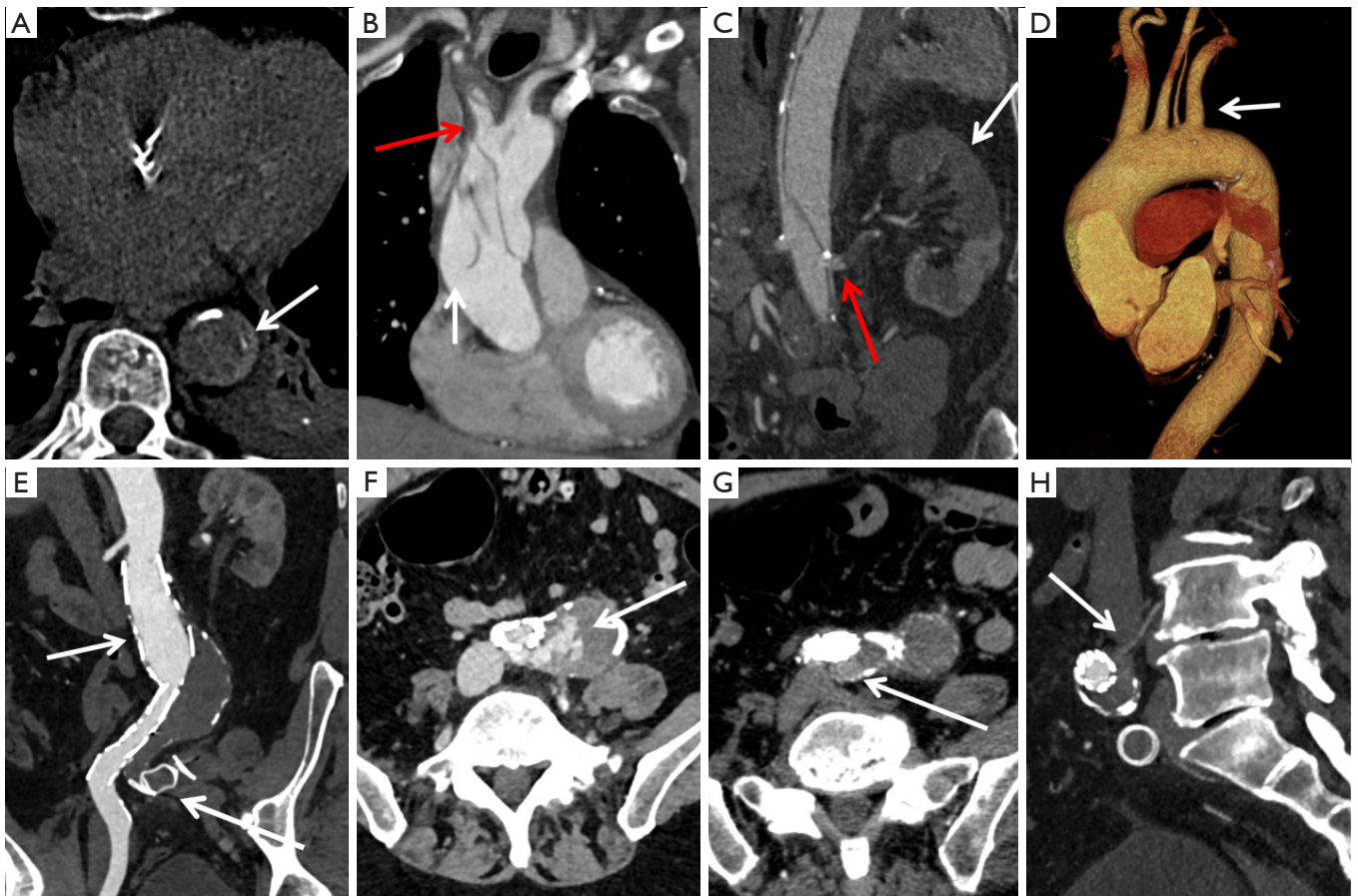


Figure 1 Multiphase acquisition for aorta. Noncontrast image (A) demonstrates crescentic hematoma with displacement of intimal calcification. Sub-millimeter resolution arterial phase acquisitions are useful for definition of anatomy. (B) and (C) demonstrate a dissection flap in the ascending and descending thoracic aorta. The arterial phase CT image (B) is accurately depicting the entry tear (white arrow), arch vessel involvement (red arrow) and (C) is depicting the extension in the left renal artery (red arrow) with hypoperfusion of the superior pole of the left kidney (white arrow; lower pole is spared by perfusion through inferior polar artery). Volume rendered image (D) from a different patient shows an anatomical variant with a four-vessel arch. The delayed images are useful for the detection of endoleak in post-endovascular repair. Figure (E) demonstrates an arterial phase acquisition in a patient with aorto-right iliac stent-graft and amplatzer plug occlusion of left common iliac artery. The delayed phase image (F) demonstrates contrast pooling in the excluded sac. Corresponding arterial phase image (G) shows only a subtle hyperdensity in the sac and a reformatted arterial phase image demonstrates the source of the endoleak from a lumbar artery (H).

Aortic CTA protocols

A typical aortic CTA protocol includes multiphase acquisition. At our institution, the standard is a three-phase examination with non-contrast, arterial and delayed phase imaging (Figure 1).

Non-contrast CT: a non-contrast phase is particularly useful in patients with suspected acute aortic syndrome to evaluate for the presence of aortic intramural hematoma. Non-contrast images are also useful in differentiating calcifications

and surgical graft material from peri-prosthetic contrast enhancement or graft leak. The radiation dose of non-contrast phase is kept low by using wider collimation and low tube potential with concomitant reduction in tube current.

CTA: non-gated thoracic aortic CTA is usually performed with a collimation of 0.5 to 1.0 mm, pitch of 1 to 1.5 mm, and reconstruction of 1.0 to 1.5 mm slices with 0.75 to 1 mm inter-slice gap. A tube potential of 120 kVp is routinely used, although a lower kVp (70–100 kVp) may be used in small sized individuals. Automated tube current modulation

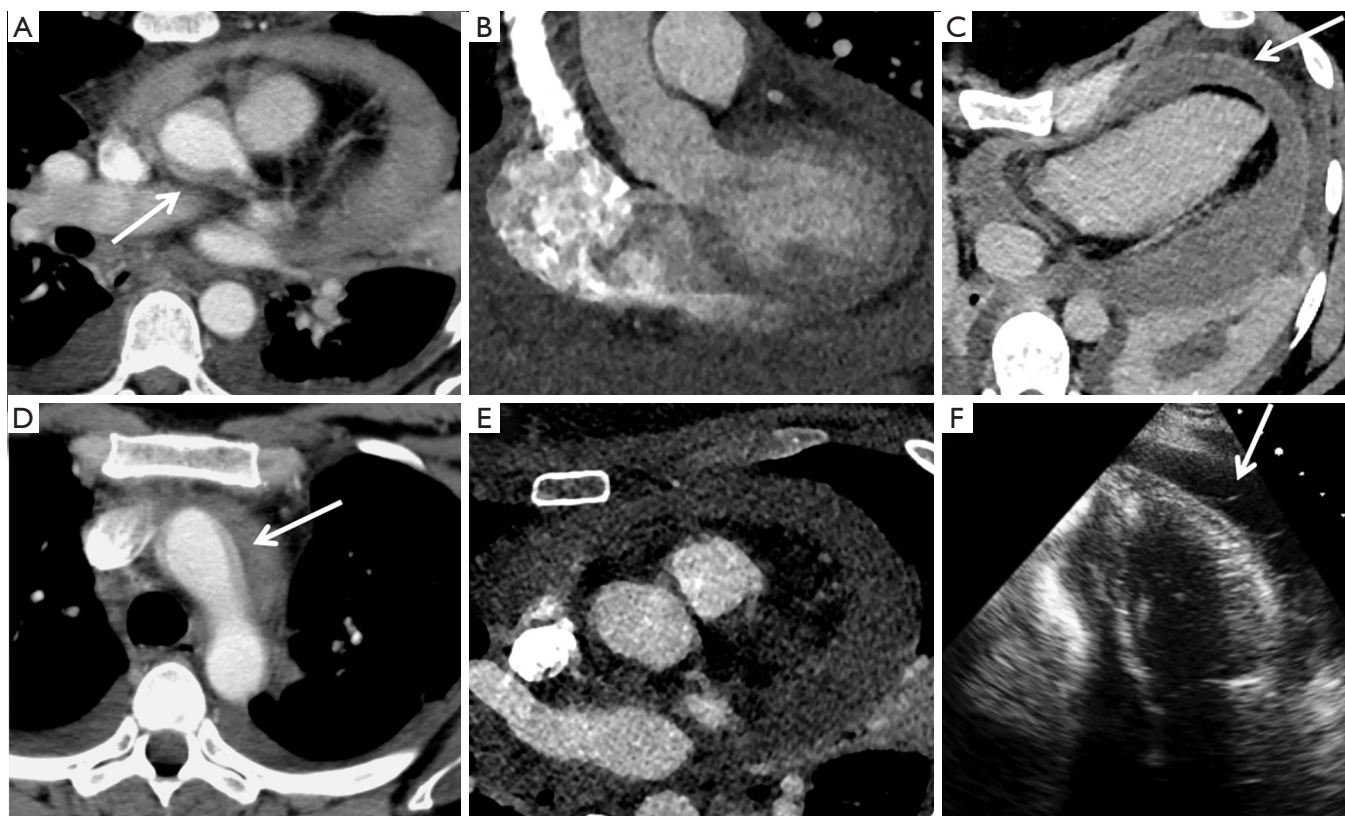


Figure 2 Gated vs. non-gated acquisitions for aortic root. 36F with Ehlers-Danlos (hypermobility genetic variant) was hospitalized with severe neck and back pain. A non-gated CT angiogram (A,B) showed a hyperdense pericardial effusion and possible flap (arrows) suggesting type A aortic dissection. She underwent a pericardiocentesis which found hemorrhagic fluid. Repeat gated imaging was negative for dissection (C,D) and revealed stable pericardial effusion. A delayed phase image was included in the second exam (E) which demonstrated the circumferential pericardial thickening and enhancement. Echocardiography demonstrated pericardial fluid with fibrinous strands (F) and a diagnosis of hemorrhagic pericarditis was made. She had a negative extensive work up for infection and autoimmune disease. Patient improved with colchicine/NSAIDs and a final clinical diagnosis of viral pericarditis was made.

should be used when available. Iodinated contrast is injected at a rate of 3–5 mL/s and the overall contrast volume used is proportional to the scan time (injection rate multiplied by scan duration +5 to 10 seconds). Reconstructions with small field of view are used when relevant for higher spatial resolution. A full field of view must be reconstructed for all acquisitions to detect incidental findings. Examination of the thoracic aorta often includes the evaluation of the abdominal aorta and iliac arteries because of high risk of involvement of these vessels and to facilitate treatment planning. Abdominal aortic CTA may be limited to the abdomen and pelvis. Cardiac motion can result in significant artifact in the aortic root and ascending aorta and can impact the accuracy of aortic measurement or even mimic dissection. Electrocardiogram (ECG) gating can mitigate these issues

and is increasingly utilized when aortic root abnormality or ascending aortic dissection is suspected (*Figure 2*).

Delayed scan: delayed images of the aorta are routinely acquired 2 minutes after injection at our institution to assess the venous structures as well as late filling of a false lumen in dissections, slow endoleaks, or contrast extravasation from aortic rupture (1).

Split bolus technique & DECT to minimize radiation exposure

The use of medical imaging involving ionizing radiation has increased tremendously over the past few decades with CT imaging accounting for roughly half of all the medical radiation exposure in United States (1-5). There is

a growing awareness in the medical community of potential cumulative radiation associated health risks to patients requiring serial imaging exams (6-8). Patients with a history of endovascular aortic repair (EVAR) undergo routine surveillance CTA for detection of endoleak and repeated three phase scans increases these patients' risk of receiving a high lifetime cumulative radiation burden. Available literature suggests that late ruptures are very rare in cases of type II endoleaks and some authors recommend only an arterial phase for routine follow-up without a routine delayed phase acquisition (9,10). Considering these issues, there has been on-going debate about the ideal CT protocol for endoleak detection spurring research into reducing radiation exposure without losing the clinical information provided by a typical triple phase scan. Early experience with incorporation of dual energy CT (DECT) and split-bolus protocols into CTA has shown promise (10-12).

Using DECT, Flors *et al.* conducted a blinded triple read-out study for thoracic aortic aneurysms after a triple phase acquisition including polychromatic beam unenhanced, a polychromatic beam arterial phase and dual-energy 300-second late delayed phase acquisitions. Blinded review during three reading sessions included session A (standard triple phase images), session B [virtual non-contrast (VNC) and late delayed phase; equivalent to a single-phase scan], and session C (VNC, arterial phase, and late delayed phase; equivalent to a dual phase scan). The sensitivities of sessions B and C were 85.7% and 100% respectively, using session A as a reference standard. Based on these observations, the authors propose that the use of dual-phase or single-phase protocols may result in radiation dose reduction of 19.5% and 64.1%, respectively (11). In a similar study design for abdominal aortic aneurysms, Stolzmann *et al.* reported 100% sensitivity for endoleak detection on readouts equivalent to sessions B & C in study by Flors *et al.* (12).

Javor *et al.* successfully applied the split bolus technique with iodinated contrast material injected in two phases and image acquisition while the second bolus is in arterial phase. The first bolus was timed in such a way that it was within the venous phase at the time of acquisition to allow filling of slow flow leaks (10,11). If this split-bolus technique were combined with a dual energy technique, theoretically even the non-contrast phase could be omitted and replaced by VNC images (10,11). The authors reported that a single acquisition split bolus technique with DECT allowed radiation dose reduction of up to 42% (10) with comparable image quality and good diagnostic accuracy (endoleak detection rate of 96%) (10). An important disadvantage

of this strategy, however, is lack of dynamic angiographic information on a single phase. In equivocal cases with a question of type II *vs.* III endoleaks, the kinetics of the contrast spread between the arterial and venous phases can be helpful in identifying the source of leak. Another potential drawback in scenarios where a CTA is done very early (<1 week) after an endovascular procedure is that the contrast remaining in the aneurysm sac from the procedure might be mistaken for active leakage (12). Another potential pitfall is the limited dual energy field of view in dual-source DECT scanners; careful centering of patient is also important to avoid suboptimal VNC images (11).

Whole body CTA with high-pitch dual source CT

Modern wide detector systems with fast gantry rotation and dual-source tube arrangements allow for extremely short image acquisition time such as whole body aorta examination in 3 seconds. Due to their speed, these acquisitions are less prone to motion artifacts at the aortic root and the ascending aorta. Modern CT technology has achieved such high temporal resolution that scanners can virtually freeze motion for the evaluation of the thoracic aorta without ECG-gating. Third generation dual-source CT allows pitch values of up to 3.4 and motion free images of the aortic root can be acquired with or without electrocardiographic gating (13,14) (*Figure 3*). Beers *et al.* reported that both ECG-gated and non-ECG-gated high-pitch protocols provide equivalent subjective and objective image quality without motion related artifacts. The aortic roots were reliably evaluable in all patients and vascular contrast was excellent (15). High-pitch technique requires adjustments to be made in bolus timing and triggering in order to attain a homogenous and optimum [>200 Hounsfield units (HU)] aortic enhancement. Beers *et al.* reported that a start delay of 10 seconds after a trigger threshold of 140 HU in a region of interest placed in the descending aorta allows for homogenous and adequate contrast enhancement along the entire aorta (15,16). In the non-ECG-gated mode, the scan is triggered manually by the CT technician irrespective of the cardiac cycle. In the ECG-gated mode, the scan is triggered automatically by the scanner, usually in diastole (15).

An advantage of high speed ECG-gated imaging is the potential opportunity for simultaneous coronary artery assessment. Using a 128-detector row, dual-source CT scanner and ECG-synchronized high-pitch CTA (pitch 3.2), Goetti *et al.* reported diagnostic image quality for 97.2% of

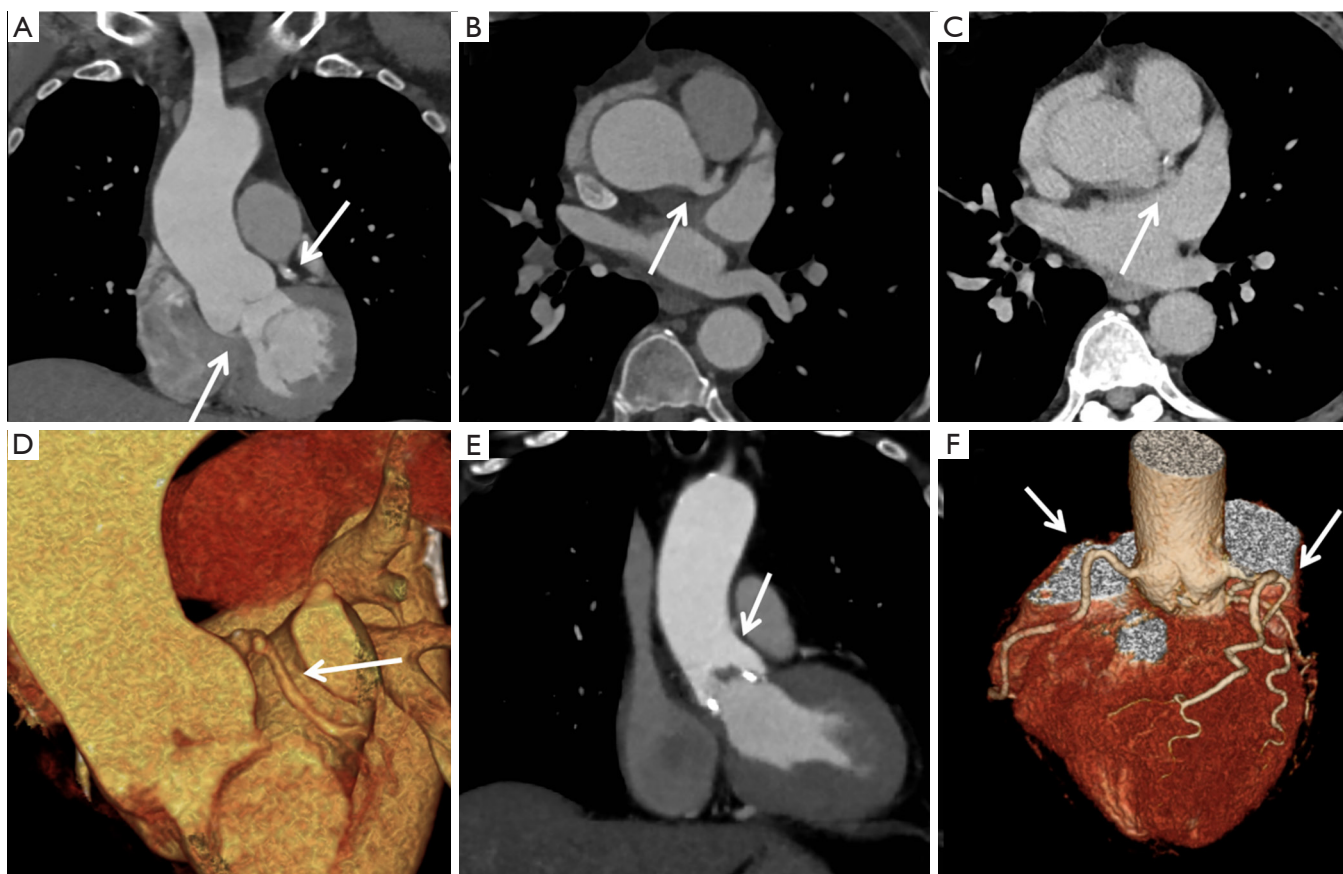


Figure 3 High pitch helical imaging. Thoracic CTA image (A) with a 192 row detector dual source scanner with a motion-freezing helical pitch of 1.7 illustrates good definition of the aortic root and the proximal segments of the coronary arteries (B). Corresponding venous phase acquisition with a pitch of 1 shows motion blurring at the root and coronary ostium (C). Volume rendered image (D) demonstrates the course of the left main and proximal circumflex coronary artery. Non-gated high pitch helical acquisition from a different patient with aortic valve endocarditis shows vegetation in relation to the leaflet of bioprosthetic aortic valve (E). Volume rendered image from a gated-high pitch helical acquisition (F) demonstrates the diagnostic quality definition of the coronary arteries.

coronary artery segments in 83% of patients. The authors conclude that at an average heart rate less than 63 beats per minute with minimal heart rate variability, diagnostic evaluation of the coronary arteries can be achieved at a low radiation dose simultaneously with aortic CTA (2.3 ± 0.3 mSv for thoracic and 4.4 ± 0.5 mSv for thoracoabdominal) (17). Limitations of this study include that it was performed without control subjects and the diagnostic performance of coronary CTA was not assessed.

Low dose TAVR CTA

Aortic valve stenosis is a common cause of morbidity and mortality in the aging population in the United States.

TAVR is a novel treatment method for treating many of these patients who are high risk candidates for open surgical valve replacement (18). A pre-procedural CTA allows for annulus sizing, device selection, evaluation of suitability of the peripheral arteries for access, as well as selection of appropriate fluoroscopic projections and is considered vital for procedural success of TAVR (19). Candidates for TAVR often have co-morbidities such as chronic renal failure that can adversely impact outcomes (20-22). There has been ongoing debate about the actual incidence, significance and even existence of acute kidney injury following intravenous iodinated contrast media injection during CT (23-27). However, current guidelines recommend careful or limited use of iodinated contrast in patients with renal dysfunction

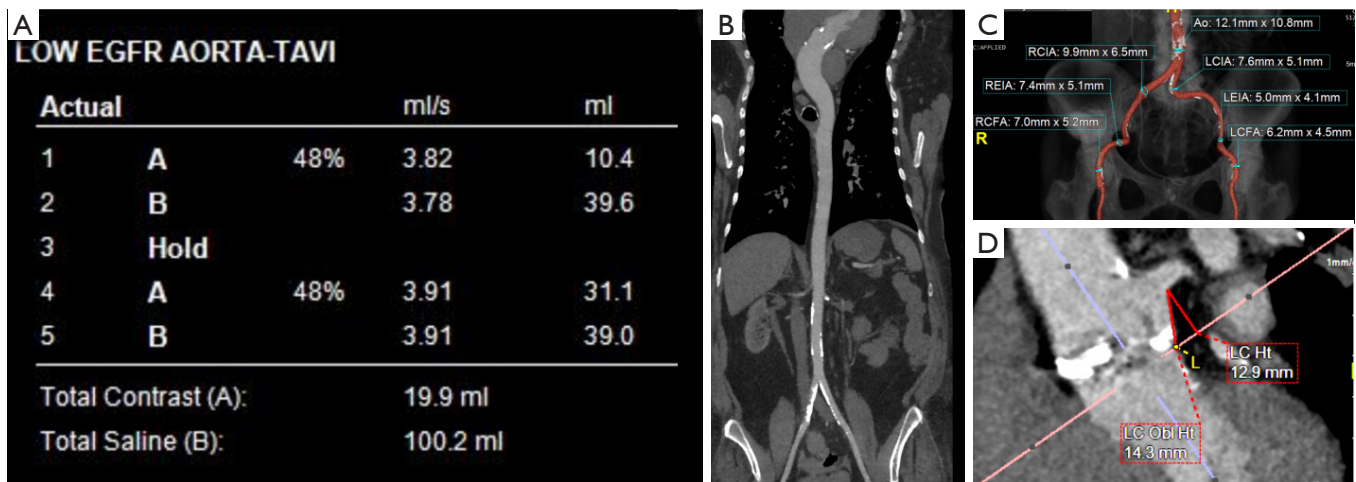


Figure 4 Gated aortic imaging for TAVI planning. Chart (A) shows the injection protocol with 10.4 cc test bolus with a 48% solution of iodinated contrast followed by a prospective gated high pitch helical acquisition of the thoraco-abdominal aorta and iliac vessels (B) with 31.1 cc of 48% solution of iodinated contrast. The study was performed by a total contrast volume of 19.9 cc (41.5 cc of 48% diluted contrast solution) and the attenuation values at the aortic root and iliac vessels were 180 and 168 HU respectively. A volume rendered image from a different patient (C) demonstrates diagnostic quality images for iliac measurements. The curved MPR image (D) demonstrates aortic root anatomy. TAVI, transcatheter aortic valve implantation.

whose risk for AKI is significant ($GFR < 30 \text{ mL/min/1.73 m}^2$) or borderline ($GFR < 45 \text{ mL/min/1.73 m}^2$) (28), and reduction of contrast agent volume is desirable in patients with chronic renal failure.

An ultra-low contrast dose pre-procedural TAVI is feasible with modern dual-source CT systems using prospectively ECG-triggered high-pitch helical acquisition. Bittner *et al.* reported good to excellent image quality with mean attenuation of 285 ± 60 and 289 ± 74 HU at the aortic annulus and iliac bifurcation respectively. The average iodinated contrast material (Iomeron 350) dose used in this study was 38 mL compared to a reference range of 80 and 120 mL for routine dose pre-TAVR CTA (20,29). Scan parameters included tube voltage 100 kV, 350 mAs, $2 \times 192 \times 0.6 \text{ mm}^3$ collimation, 250 ms rotation time and a pitch of 3.2. A test bolus of 8 mL of contrast was used for assessing the bolus transit time and 30 mL (at 4 mL/s) contrast with 40 cc saline chase was used for subsequent CTA. Procedural success was achieved in 31 out of 35 patients who underwent TAVI following the low-dose planning scan (20). A drawback of this technique is single-phase evaluation of the aortic annulus as opposed to using the largest systolic phase available on a multiphase acquisition; re-sizing the annulus via transesophageal echocardiography at the time of the procedure can mitigate this disadvantage.

There have been other reports of use of ultra-low volume contrast agent (20–30 mL) for TAVR planning (30–33) also utilizing high pitch dual source scanning, however these studies were either done on a small patient population or did not include the evaluation of the procedural success of the following TAVR procedure. Other approaches for a low dose pre-TAVR scan include invasive methods with contrast injection via pigtail catheters placed in the pulmonary artery and/or aorta (34–36). Joshi *et al.* (34) and Zemedkun *et al.* (36) reported ilio-femoral CTA assessment with 10–15 mL and 23 cc of contrast agent (respectively) injected via pigtail catheter in the infrarenal abdominal aorta. These techniques are, however, invasive and assessment limited to the iliofemoral arteries, excluding imaging of the aortic root which is essential for device selection (34–36). Another potential technique for contrast dose reduction is using low keV reconstructions on dual-energy CT; while there is published data on low dose coronary/pulmonary CTA with this technique (37,38), there is no published experience with pre-TAVR scanning and one study reported that image quality was impacted (37). Overall, high-pitch ECG-triggered helical imaging is a reliable and reasonable approach for low-contrast dose pre-TAVR scanning and is routinely performed at our institution with a total of 30–40 cc of contrast (Figure 4).

MR angiography of the aorta

Magnetic resonance angiography (MRA) has become a dominant option for noninvasive imaging of the aorta owing to its comprehensive multiplanar endoluminal evaluation and excellent soft tissue contrast for mural evaluation. MRA has become the preferred modality for aortic imaging for patients in whom the goal is to avoid the use of iodinated contrast material or ionizing radiation. Moreover, MRA can provide functional data such as flow volume and velocity, a major advantage compared to CTA. Drawbacks to MRA include incompatibility with certain implantable medical devices, and difficulty for patients with claustrophobia or who cannot tolerate lengthy exams. There is a wide spectrum of indications for MRA of the aorta (39), including acute aortic syndrome (aortic dissection, intramural hematoma, penetrating atherosclerotic ulcer, aortic aneurysm), post-operative aortic repair surveillance after open or endovascular treatment, congenital heart disease (including aortic coarctation and bicuspid aortic valve, vasculitis, and connective tissue disorders such as Marfan's or Ehlers Danlos syndromes). ECG gating can help minimize motion artifact when performing MRA of the thoracic aorta, particularly at the aortic root, but is not necessary for the abdominal aorta. MRA can be performed with an intravascular gadolinium-based contrast agent, or without contrast.

Although noncontrast MRA has become easier to acquire with newer techniques, contrast enhanced MRA (CE MRA) remains the first line technique in suitable patients (40). This is partly due to its superior speed and independence of flow dynamics which allows CE MRA to avoid many of the artifacts that plague noncontrast MRA. CE MRA achieves excellent contrast-to-noise ratio by utilizing an intravenous injection of an extracellular gadolinium chelate, which dramatically shortens the T1 relaxation times of protons in blood. With the transition from using 1.5T to 3.0T magnets, the increased signal to noise ratio (SNR) can be used to lower the contrast agent dose and achieve the same image quality (41). Studies have shown for example that a contrast dose reduction from 0.15 to 0.05 mmol/kg did not adversely affect image quality or spatial resolution when evaluating the supra-aortic arteries (42).

One of the salient features of CE MRA is the need to acquire images in a small window of time while there is first pass arterial enhancement after the administration of contrast and before the appearance of venous contamination. 3D gradient recalled echo (GRE) sequences are commonly used for CE MRA since they provide

a favorable balance of speed, SNR, spatial resolution, and background suppression. Minimizing flip angle (25–45 degrees), TR (<5 ms) and TE (<3 ms) all help to minimize acquisition time in 3D GRE sequences for CE MRA (40). The need to acquire images in such a small window of time can make it difficult to achieve desirable spatial resolution and result in inadequate image quality. More recent contrast agents such as Gadofosveset (AblavarTM or VasovistTM) have addressed this issue by having a much longer intravascular circulation time with higher relaxivity, which allows for longer scan times to achieve better spatial resolution. For instance, a study using 10 mL of Gadofosveset trisodium demonstrated qualitatively better image quality compared to 30 mL of gadopentetate dimeglumine (43).

One of the crucial breakthroughs which allowed high SNR images to be acquired quickly for MRA was the development of parallel imaging, which includes acquisition and reconstruction methods such as SMASH (SiMultaneous Acquisition of Spatial Harmonics) (44), SENSE (SENSitivity Encoding) (45), and GRAPPA (GeneRalized Autocalibrating Partially Parallel Acquisitions) (46). By utilizing phased array RF coils, parallel imaging accelerates acquisition time by encoding additional k-space lines for each line encoded by the magnetic field gradients, with acceleration factors ranging from 2–32 (47). The degree of acceleration is dependent on the degree of SNR that the imager is willing to trade off in the interest of decreased scan time. The benefits of parallel imaging have been accentuated by the transition to higher field 3T scanner which provide greater SNR to sacrifice.

CE MRA protocols typically include a pre-contrast test 3D dataset, which can ensure accurate position, search for detrimental artifacts, and to use as baseline data for subtraction to enhance vessel visualization (Mask Mode subtraction). At least two post-contrast datasets are then acquired, with an interval of approximately 10 seconds between the two during which the patient can freely breathe. Additional post contrast datasets help visualize structures such as large aneurysms which have slow flow, compensate for variable flow dynamics based on patient cardiac output, allow visualization of venous structures, and can be used for dynamic perfusion data (47). While CE-MRA mainly evaluates vascular lumen, MRA protocols for the aorta should include sequences to visualize vessel walls such as T1-weighted spin echo in the axial plane. When imaging the abdominal aorta, fat suppression can be used to improve wall visualization. When evaluation of

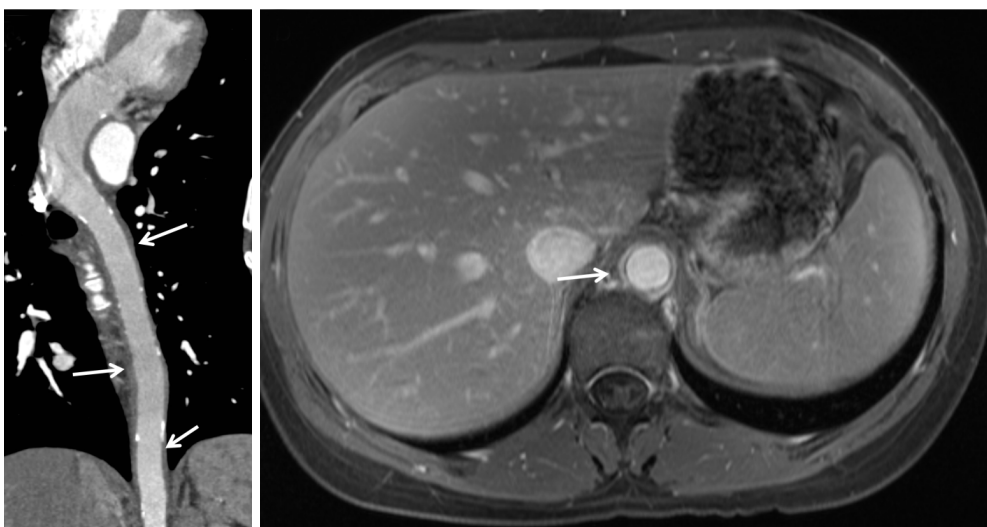


Figure 5 Curved MPR aortic CTA image from a patient with giant cell arteritis shows diffuse aortic wall thickening (arrows). The VIBE sequence after giving contrast can evaluate for mural enhancement which is a sign for disease activity in vasculitis.

enhancement is desired, a high resolution isotropic sequence such as Volume Interpolated Breath-hold Examination (VIBE) utilizing a lower flip angle (10–15 degrees) can be used (40). The VIBE sequence after giving contrast can evaluate for mural enhancement or enhancement of tumor thrombus (*Figure 5*).

Although gadolinium-based contrast agents (GBCAs) do not confer the risk of nephrotoxicity that iodinated contrast agents do, there have been rare case reports showing that use of gadolinium in patients with renal failure can result in nephrogenic systemic fibrosis. The risk of NSF is higher with linear agents as compared to macrocyclic GBCAs. In addition, there are rising concerns for long term tissue retention of GBCAs in the human body, specifically in the brain, even in individuals with normal renal function (48-52). The structure of the GBCA again impacts the degree of brain accumulation and linear GBCAs have significantly higher accumulation compared to macrocyclic agents (49,53). Due to these considerations, the imager should always consider FDA label indications and dosing schemes. When GBCAs are indicated, the use of a macrocyclic GBCA (e.g., gadobutrol, gadoteridol, or gadoterate meglumine) should be considered rather than a linear agent. For patients with documented allergy to macrocyclic agents, it is appropriate to use linear agents if indicated (51).

The risk of NSF, along with the need for adequate breath holds by patients for CE MRA, has contributed to the development and use of a range of non-contrast MRA

techniques (NC MRA) for evaluation of the aorta. Common NC MRA techniques include time of flight (TOF), steady-state free precession (SSFP), and phase contrast (PC). While the physics of each sequence is beyond the scope of this review article, a brief discussion of their utility and drawbacks is worthwhile.

The initial technique for NC MRA was time of flight imaging which relies on the inflow effect of blood. Repeated radiofrequency (RF) excitation is applied to a slice of interest to saturate the spins of stationary tissue, and inflowing blood which has not been exposed to the repeated RF will have fresh longitudinal magnetization resulting in high signal intensity (54). Sequences with a short repetition time (TR) will maximize flow related enhancement (47). The thickness of the imaging slice should be kept to a minimum and be oriented perpendicular to the direction of flow, to minimize artifactual loss of signal for in-plane flow. To avoid signal loss related to dephasing from turbulent flow, TOF utilizes a flow-compensated readout (55). To suppress signal from flow within venous structures, a saturation pulse can be applied to eliminate signal in the direction of venous flow (56).

Steady state free precession imaging leverages high SNR which relies on inherent T2 and T1 signal rather than inflow to image the aorta without contrast. 2D SSFP was first developed but often has problematic out-of-slice contributions, with suboptimal voxel resolution (57). The development of 3D SSFP greatly minimized these



Figure 6 Free breathing 3D SSFP utilizing a diaphragm navigator sequence (A) from a patient with type B intramural hematoma (white arrows) demonstrates the anatomy of the aortic arch (red arrow). T1W black blood image (B) shows a hyperintense IMH (arrow). 3D SSFP MRA may provide better measured SNR and CNR compared to CE MRA, with higher image quality of the aortic root (C) and proximal coronary arteries (D). Axial T1 weighted black blood image from a patient with post root repair type A aortic dissection shows a flap (E) in the aortic arch that extends to the arch vessels (F). Contrast MRA images further depict the dissection flap in the arch extending to proximal innominate artery (G,H).

shortcomings to become a valuable NC MRA technique (Figure 6). In patients who cannot perform breath holds, 3D SSFP can acquire images during free breathing utilizing a diaphragm navigator sequence. In some studies, 3D SSFP MRA has actually been demonstrated to provide better measured SNR and CNR compared to CE MRA, with higher image quality of the aortic root (57). One of the drawbacks to 3D SSFP, particularly at 3T, are off resonance artifacts which can manifest as dark bands traversing the images and possibly mimic aortic dissection. This artifact can be minimized by using small volume frequency scouting to select the optimal frequency (58).

Phase contrast MRA (PC MRA) is a non-contrast technique with the unique capability to quantify blood flow and velocity. PC MRA utilizes paired bipolar gradient lobes to depict a phase shift present in the magnetic spins within flowing blood which is proportional to velocity (59). While spins within

stationary tissue should not develop a net phase shift, spins moving along (or opposite to) the direction of the magnetic field will develop a phase shift which can be translated to signal proportional to velocity. By allowing for velocity measurements, pressure gradients can be calculated utilizing Bernoulli's equation, $P_{\max} = 4 \times V_{\max}^2$. Such measurements are useful in adding physiologic information to the anatomic information provided by other MRA techniques, such as determining severity of an aortic coarctation or degree of aortic valve stenosis or regurgitation.

Positron emission tomography (PET)

Indications for aortic PET

^{18}F -fluorodeoxyglucose-positron emission tomography (^{18}F -FDG-PET) uptake within tissue provides metabolic

information which can indicate activity related to inflammation or neoplasia. For improved anatomic signal localization, ^{18}F -FDG-PET is generally combined with a cross-sectional imaging modality, most commonly CT. Protocols for aortic ^{18}F -FDG-PET/CT imaging typically involve administration of ^{18}F FDG after an overnight fast and imaging 90–180 min after FDG administration. The acquisition of CT and PET components of the ^{18}F -FDG-PET/CT are non-simultaneous (60). FDG uptake measurements of the aorta are reproducible on serial imaging (61). Aortic ^{18}F -FDG-PET/CT imaging has been tested for its utility for vascular graft infection, large vessel vasculitis, detection of atherosclerotic plaque inflammation, and prediction of outcome in aortic aneurysms.

Aortic prosthetic graft infections are a challenging clinical problem which can difficult to diagnose on conventional imaging, especially in the chronic setting (62,63). Infected vascular grafts warrant surgical removal and accurate diagnosis is essential to avoid unnecessary major surgery associated with high risk for morbidity (62,64). Aspiration and culture is considered gold standard, however a perigraft abscess or fluid collection may not be always present or might not be suitable for percutaneous aspiration (62,64). CTA and MRA may be useful in diagnosing graft infection in cases with typical imaging findings of graft related abscesses; however, these modalities lack specificity and might result in unnecessary major surgeries. Combining the anatomical information obtained by CT with the increased metabolism on PET significantly improves the diagnostic accuracy and decreases the rate of false-positives (64). Semi-quantitative PET-CT evaluation using the maximal standardized uptake value (SUVmax), tissue-to-background ratio (TBR), and visual grading scale (VGS) has high sensitivity (up to 91%) and specificity (up to 93%) for vascular graft infections (65,66). ^{18}F -FDG-PET/CT has also been reported to be useful for detection of infections related to pacemaker-leads and transcatheter or surgically implanted aortic valves (67,68). These are mostly case reports with no reproducible evidence as yet regarding their additional utility over cardiac ultrasound/CTA.

Takayasu arteritis (TA) and giant-cell arteritis (GCA) and are the most common large-vessel vasculitides (LVV) and often involve the aorta. Imaging studies are increasingly used for the diagnosis and for the monitoring of the disease activity in LVV. On CT and MRI, increased vessel wall thickness, vessel wall edema, and mural enhancement are

considered signs of active disease. Active inflammatory versus chronic fibrotic wall thickening require different management and can be difficult to discriminate on CT and MRI. The metabolic information provided by PET is a potentially more accurate marker of disease activity in LVV (69). Linear, smooth mural FDG uptake extending over long vessel segments is typically seen in active LVV (69) (*Figure 7*). A positive ^{18}F -FDG-PET/CT is also associated with a higher risk of aortic complications in patients with GCA (70). ^{18}F -FDG-PET alone or in combination with CT has high accuracy in the diagnosis of large-vessel inflammation in both GCA (sensitivity 90% and specificity 98%) and TA (sensitivity 84% and specificity 84%) (71). FDG tracer uptake can also be observed in patients without biochemical markers of LVV disease activity, which could potentially reflect subclinical inflammation that could be a marker for increased risk of disease progression or vascular complications. The clinical value of this finding is however as yet poorly understood and requires further attention and research (71). ^{18}F -FDG-PET/CT is also useful in diagnosis of IgG4-related related aortitis and periaortitis (72,73).

Risk of rupture is a major concern in patients with aortic aneurysms and requires serial imaging follow up for detection of early indicators of rupture to facilitate a timely intervention. Aortic FDG uptake has also attracted research interests for predicting the risk of adverse outcome in aortic aneurysms and its performance has been evaluated in several studies (74-77). A recent systematic review evaluated the performance of aortic ^{18}F -FDG-PET/CT by pooling the results of various PET-CT studies (78). Authors conclude that the evidence provided by these studies is contradictory; results vary widely from significant negative correlations to non-significant positive associations between ^{18}F -FDG uptake and AAA growth. At the present time, ^{18}F -FDG-PET/CT is not recommended for use as a growth or rupture prediction tool in routine practice (78).

Early work on ^{18}F -FDG-PET/CT revealed the presence of focal vascular FDG uptake unrelated to calcified plaques in patients undergoing PET-CT for malignant conditions (79), suggesting that it may possibly be located in areas of metabolically active atherosclerosis. The first clinical prospective arterial ^{18}F -FDG-PET/CT study by Rudd *et al.* established that FDG tracer uptake was increased in carotid atherosclerotic plaques (80). Atherosclerosis is characterized by a spotty pattern corresponding to areas of macrophage infiltration (79,81,82) that are the histological hallmark of plaque inflammation (83,84). Inflammation plays a crucial role in the progression of atherosclerotic

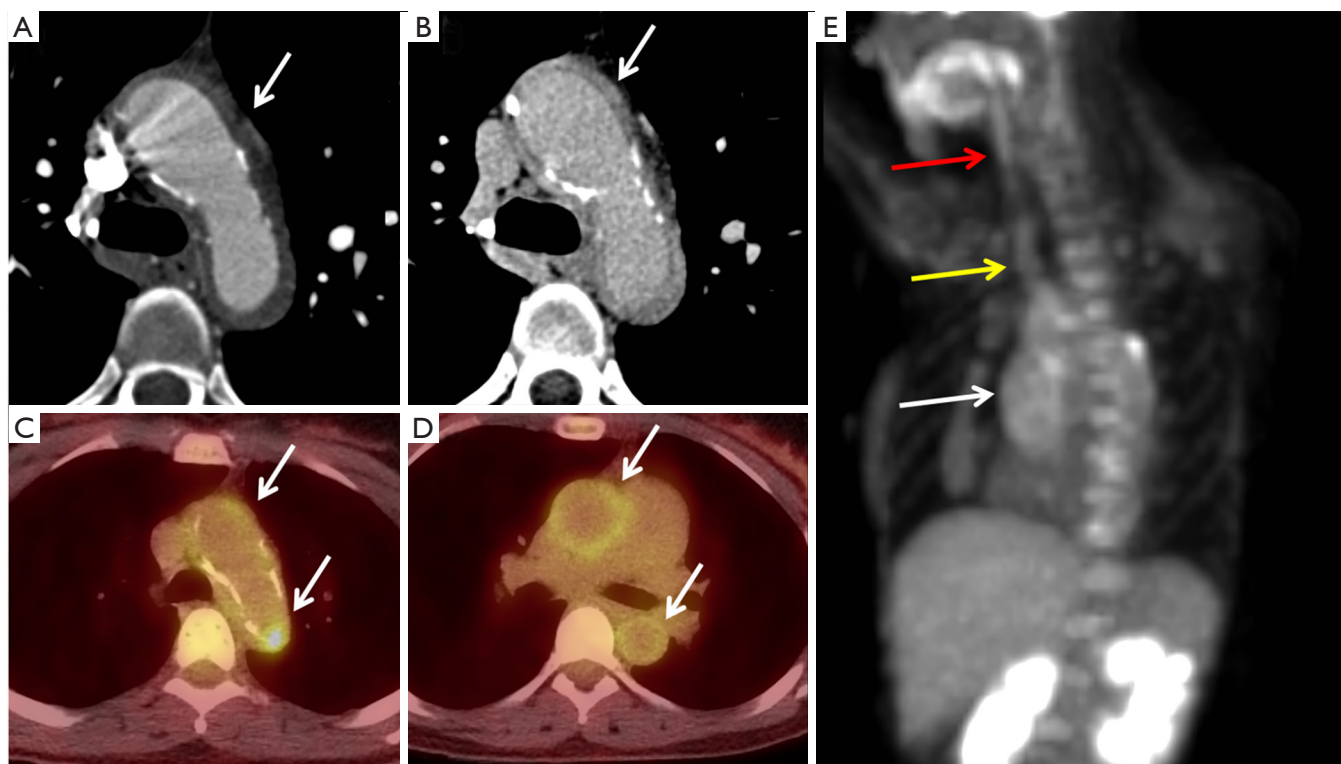


Figure 7 CTA arterial (A) and delayed (B) images from a patient with takayasu arteritis demonstrate diffuse aortic wall thickening with delayed enhancement. ^{18}F -FDG-PET/CT images (C,D) demonstrate the diffuse long segment uptake involving ascending through descending aorta (arrows). MIP image from the same study redemonstrates the aortic uptake (white arrow) and also demonstrates the diffuse uptake in the innominate (yellow arrow) and right carotid (red arrow) arteries (E).

disease (60,83,85). Aortic ^{18}F -FDG uptake strongly predicts cardiovascular events, independent of traditional risk factors (86). ^{18}F -FDG uptake within the plaques has also been used to assess the response to pharmacological interventions. Statin therapy produces significant rapid dose-dependent reductions in aortic and carotid ^{18}F -FDG uptake potentially representing decreases in atherosclerotic plaque inflammation (87). Despite these advancements, the use of ^{18}F -FDG-PET/CT remains largely restricted to research domain with no current application in clinical atherosclerotic imaging. The limited spatial resolution of current PET imaging systems, PET-CT image misregistration and image degradation by cardiac motion are important factors limiting the clinical utility of this modality (60).

Positron emission tomography-magnetic resonance angiography (PET-MRA)

Magnetic resonance imaging (MRI) has been introduced

recently as part of hybrid PET/MRI systems and offers several advantages over PET/CT systems in the evaluation of vascular inflammation. PET/MRI systems result in less ionizing radiation exposure and allow simultaneous acquisition of MRI and PET images resulting in better co-registration and motion correction (60). In addition, anatomic features of vulnerable plaques on MRI (necrotic core, fibrous cap thickness, plaque hemorrhage) are complementary to the functional information provided by PET (88,89). Experience with and scientific evidence for the clinical utility of aortic PET-MRA remains limited (60) and is covered in greater detail elsewhere in this issue.

Potential role of ultrasound in post-EVAR aortic imaging

As discussed earlier, CTA is the standard surveillance method after endovascular abdominal aortic aneurysm repair. Along with many advantages, CTA is also associated

with health-care costs and potential risks from radiation and intravenous contrast exposure. Abdominal ultrasound has been used as a screening tool for the evaluation of clinically suspected abdominal aortic aneurysm and for screening evaluation for abdominal aortic aneurysm in elderly individuals with cardiovascular risk factors (90). Since 2009, the Society for Vascular Surgery has advocated the use of annual surveillance with ultrasound after the first post-operative year for uncomplicated abdominal-EVAR. Per exam cost of ultrasound is very low compared to a CTA (US \$234 *vs.* \$2,132) and if applied widely has a potential for substantial health care cost reduction (91).

The diagnostic accuracy of CEUS in post-EVAR abdominal aneurysm has been found to be superior or at least non-inferior to CTA based on data from several studies and meta-analyses (92-97). Cross-modality aneurysm diameter measurements correlate very well with a minimal difference (mean difference 1.70 mm; more on CTA). CEUS is highly sensitive for endoleaks (92). A recent systemic review pooling data from 31 different studies comparing paired CTA and ultrasound scans, reported that CTA had a higher sensitivity for endoleak detection compared to duplex ultrasound (DUS) (214/2,346 on CTA *vs.* 77/2,346 for DUS), however CEUS was more sensitive for endoleak detection than CTA (138/1,694 *vs.* CTA 51/1,694). Although, CEUS was no better (but also non-inferior) for the detection of type I and III endoleaks (that require corrective measures) (92).

It is important to note that CEUS, especially if performed by an unskilled user, could miss graft stenosis, migrations, dislocations and endoleaks (98). In standard clinical practice, very few sonographers are trained in the use of CEUS in the aorta. Another potential caveat of ultrasound imaging is the limited image quality in obese patients. CEUS is a promising and evolving modality for the follow-up of uncomplicated EVAR for abdominal aorta but as of yet is limited in clinical use.

Conclusions

Modern CT scanners with wide detector array, rapid gantry rotation and high helical pitch allow for low contrast and radiation dose CT angiography, result in less cardiac-motion related artifacts, have potential for eliminating the need for ECG gating in aortic application, and may provide an opportunity for simultaneous coronary assessment when ECG-gated technique is used. Split bolus technique and dual energy VNC images are useful for radiation dose

reduction without compromising the diagnostic accuracy of CTA. MRA is a useful alternative for avoiding use of iodinated contrast material and ionizing radiation. The use of 3D GRE sequences, higher relaxivity contrast agents, 3T magnets and parallel imaging methods have resulted in reduction in image acquisition time and improvement in image quality. Non-contrast MRA is a reasonable alternative for patients who cannot receive gadolinium-based contrast agents. ¹⁸F-FDG-PET/CT imaging may help avoid unnecessary surgeries in patients with suspected aortic prosthetic infection. It also provides higher specificity for detection of activity in large vessel vasculitis and has potential for detection of inflammation in vulnerable atherosclerotic plaques. CEUS is also an attractive potential imaging modality for surveillance of uncomplicated post-EVAR abdominal aorta and may have impacts on cost and radiation related health risk in the future.

Acknowledgements

None.

Footnote

Conflicts of Interest: The authors have no conflicts of interest to declare.

References

1. Mettler FA, Huda W, Yoshizumi TT, et al. Effective doses in radiology and diagnostic nuclear medicine: a catalog. *Radiology* 2008;248:254-63.
2. Hricak H, Brenner DJ, Adelstein SJ, et al. Managing radiation use in medical imaging: a multifaceted challenge. *Radiology* 2011;258:889-905.
3. Mettler FA, Bhargavan M, Faulkner K, et al. Radiologic and nuclear medicine studies in the United States and worldwide: frequency, radiation dose, and comparison with other radiation sources--1950-2007. *Radiology* 2009;253:520-31.
4. Lin EC. Radiation risk from medical imaging. *Mayo Clin Proc* 2010;85:1142-6.
5. Brink JA, Morin RL. Size-specific dose estimation for CT: how should it be used and what does it mean? *Radiology* 2012;265:666-8.
6. Brenner DJ, Hall EJ. Computed tomography--an increasing source of radiation exposure. *N Engl J Med* 2007;357:2277-84.

7. Brenner DJ, Hricak H. Radiation exposure from medical imaging: time to regulate? *JAMA* 2010;304:208-9.
8. Brenner D, Elliston C, Hall E, et al. Estimated risks of radiation-induced fatal cancer from pediatric CT. *AJR Am J Roentgenol* 2001;176:289-96.
9. Patatas K, Ling L, Dunning J, et al. Static sac size with a type II endoleak post-endovascular abdominal aortic aneurysm repair: surveillance or embolization? *Interact Cardiovasc Thorac Surg* 2012;15:462-6.
10. Javor D, Wressnegger A, Unterhumer S, et al. Endoleak detection using single-acquisition split-bolus dual-energy computer tomography (DECT). *Eur Radiol* 2017;27:1622-30.
11. Flors L, Leiva-Salinas C, Norton PT, et al. Endoleak detection after endovascular repair of thoracic aortic aneurysm using dual-source dual-energy CT: suitable scanning protocols and potential radiation dose reduction. *AJR Am J Roentgenol* 2013;200:451-60.
12. Stolzmann P, Frauenfelder T, Pfammatter T, et al. Endoleaks after endovascular abdominal aortic aneurysm repair: detection with dual-energy dual-source CT. *Radiology* 2008;249:682-91.
13. Beeres M, Schell B, Mastragelopoulos A, et al. High-pitch dual-source CT angiography of the whole aorta without ECG synchronisation: initial experience. *Eur Radiol* 2012;22:129-37.
14. Karlo C, Leschka S, Goetti RP, et al. High-pitch dual-source CT angiography of the aortic valve-aortic root complex without ECG-synchronization. *Eur Radiol* 2011;21:205-12.
15. Beeres M, Wichmann JL, Frellesen C, et al. ECG-gated Versus Non-ECG-gated High-pitch Dual-source CT for whole body CT Angiography (CTA). *Acad Radiol* 2016;23:163-7.
16. Beeres M, Loch M, Schulz B, et al. Bolus timing in high-pitch CT angiography of the aorta. *Eur J Radiol* 2013;82:1028-33.
17. Goetti R, Baumüller S, Feuchtnner G, et al. High-Pitch Dual-Source CT angiography of the thoracic and abdominal aorta: is simultaneous coronary artery assessment possible? *AJR Am J Roentgenol* 2010;194:938-44.
18. Holmes DR, Mack MJ, Kaul S, et al. 2012 ACCF/AATS/SCAI/STS expert consensus document on transcatheter aortic valve replacement. *J Am Coll Cardiol* 2012;59:1200-54.
19. Achenbach S, Delgado V, Hausleiter J, et al. SCCT expert consensus document on computed tomography imaging before transcatheter aortic valve implantation (TAVI)/transcatheter aortic valve replacement (TAVR). *J Cardiovasc Comput Tomogr* 2012;6:366-80.
20. Bittner DO, Arnold M, Klinghammer L, et al. Contrast volume reduction using third generation dual source computed tomography for the evaluation of patients prior to transcatheter aortic valve implantation. *Eur Radiol* 2016;26:4497-504.
21. Moat NE, Ludman P, de Belder MA, et al. Long-term outcomes after transcatheter aortic valve implantation in high-risk patients with severe aortic stenosis: the U.K. TAVI (United Kingdom Transcatheter Aortic Valve Implantation) Registry. *J Am Coll Cardiol* 2011;58:2130-8.
22. Arnold SV, Reynolds MR, Lei Y, et al. Predictors of poor outcomes after transcatheter aortic valve replacement: results from the PARTNER (Placement of Aortic Transcatheter Valve) trial. *Circulation* 2014;129:2682-90.
23. Davenport MS, Khalatbari S, Dillman JR, et al. Contrast material-induced nephrotoxicity and intravenous low-osmolality iodinated contrast material. *Radiology* 2013;267:94-105.
24. McDonald JS, McDonald RJ, Carter RE, et al. Risk of intravenous contrast material-mediated acute kidney injury: a propensity score-matched study stratified by baseline-estimated glomerular filtration rate. *Radiology* 2014;271:65-73.
25. McDonald JS, McDonald RJ, Lieske JC, et al. Risk of acute kidney injury, dialysis, and mortality in patients with chronic kidney disease after intravenous contrast material exposure. *Mayo Clin Proc* 2015;90:1046-53.
26. McDonald RJ, McDonald JS, Bida JP, et al. Intravenous contrast material-induced nephropathy: causal or coincident phenomenon? *Radiology* 2013;267:106-18.
27. McDonald RJ, McDonald JS, Carter RE, et al. Intravenous contrast material exposure is not an independent risk factor for dialysis or mortality. *Radiology* 2014;273:714-25.
28. ACR manual on contrast media: Version 10.2 [Internet]. 2016 [cited 2017 Jun 2]. Available online: <https://www.acr.org/~media/37D84428BF1D4E1B9A3A2918DA9E27A3.pdf>
29. Schoenhagen P, Hausleiter J, Achenbach S, et al. Computed tomography in the evaluation for transcatheter aortic valve implantation (TAVI). *Cardiovasc Diagn Ther* 2011;1:44-56.
30. Azzalini L, Abbara S, Ghoshhajra BB. Ultra-low contrast computed tomographic angiography (CTA) with 20-mL Total dose for transcatheter aortic valve implantation (TAVI) planning. *J Comput Assist Tomogr* 2014;38:105-9.

31. Felmly LM, De Cecco CN, Schoepf UJ, et al. Low contrast medium-volume third-generation dual-source computed tomography angiography for transcatheter aortic valve replacement planning. *Eur Radiol* 2017;27:1944-53.
32. Pulerwitz TC, Khaliq OK, Nazif TN, et al. Very low intravenous contrast volume protocol for computed tomography angiography providing comprehensive cardiac and vascular assessment prior to transcatheter aortic valve replacement in patients with chronic kidney disease. *J Cardiovasc Comput Tomogr* 2016;10:316-21.
33. Geyer LL, De Cecco CN, Schoepf UJ, et al. Low-volume contrast medium protocol for comprehensive cardiac and aortoiliac CT assessment in the context of transcatheter aortic valve replacement. *Acad Radiol* 2015;22:1138-46.
34. Joshi SB, Mendoza DD, Steinberg DH, et al. Ultra-low-dose intra-arterial contrast injection for iliofemoral computed tomographic angiography. *JACC Cardiovasc Imaging* 2009;2:1404-11.
35. Truong VT, Choo J, McCoy L, et al. Low-volume contrast CT angiography via pulmonary artery injection for measurement of aortic annulus in patients undergoing transcatheter aortic valve replacement. *J Invasive Cardiol* 2017;29:181-6.
36. Zemedkun M, LaBounty TM, Bergman G, et al. Effectiveness of a low contrast load CT angiography protocol in octogenarians and nonagenarians being evaluated for transcatheter aortic valve replacement. *Clin Imaging* 2015;39:815-9.
37. Raju R, Thompson AG, Lee K, et al. Reduced iodine load with CT coronary angiography using dual-energy imaging: a prospective randomized trial compared with standard coronary CT angiography. *J Cardiovasc Comput Tomogr* 2014;8:282-8.
38. Yuan R, Shuman WP, Earls JP, et al. Reduced iodine load at CT pulmonary angiography with dual-energy monochromatic imaging: comparison with standard CT pulmonary angiography--a prospective randomized trial. *Radiology* 2012;262:290-7.
39. Latson LA, DeAnda A, Ko JP. Imaging of the postsurgical thoracic aorta: a state-of-the-art review. *J Thorac Imaging* 2017;32:1-25.
40. Raptis AC. *Magnetic resonance angiography: technique*. Elsevier Health Sciences; 2013.
41. Hartung MP, Grist TM, François CJ. *Magnetic resonance angiography: current status and future directions*. *J Cardiovasc Magn Reson* 2011;13:19.
42. Tomasian A, Salamon N, Lohan DG, et al. Supraaortic arteries: contrast material dose reduction at 3.0-T high-spatial-resolution MR angiography--feasibility study. *Radiology* 2008;249:980-90.
43. Klessen C, Hein PA, Huppertz A, et al. First-pass whole-body magnetic resonance angiography (MRA) using the blood-pool contrast medium gadofosveset trisodium: comparison to gadopentetate dimeglumine. *Invest Radiol* 2007;42:659-64.
44. Sodickson DK, Manning WJ. Simultaneous acquisition of spatial harmonics (SMASH): fast imaging with radiofrequency coil arrays. *Magn Reson Med* 1997;38:591-603.
45. Pruessmann KP, Weiger M, Scheidegger MB, et al. SENSE: sensitivity encoding for fast MRI. *Magn Reson Med* 1999;42:952-62.
46. Griswold MA, Jakob PM, Heidemann RM, et al. Generalized autocalibrating partially parallel acquisitions (GRAPPA). *Magn Reson Med* 2002;47:1202-10.
47. Edelman R. *Cardiovascular magnetic resonance*. Elsevier Health Sciences; 2010.
48. Kanda T, Ishii K, Kawaguchi H, et al. High signal intensity in the dentate nucleus and globus pallidus on unenhanced T1-weighted MR images: relationship with increasing cumulative dose of a gadolinium-based contrast material. *Radiology* 2014;270:834-41.
49. Quattrocchi CC, van der Molen AJ. Gadolinium retention in the body and brain: is it time for an international joint research effort? *Radiology* 2017;282:12-6.
50. Radbruch A, Weberling LD, Kieslich PJ, et al. Gadolinium retention in the dentate nucleus and globus pallidus is dependent on the class of contrast agent. *Radiology* 2015;275:783-91.
51. Malayeri AA, Brooks K, Bryant LH, et al. NIH perspective on reports of gadolinium deposition in the brain. *J Am Coll Radiol* 2016;13:237-41.
52. Drug Safety and Availability. FDA Drug Safety Communication: FDA evaluating the risk of brain deposits with repeated use of gadolinium-based contrast agents for magnetic resonance imaging (MRI). Available online: <https://www.fda.gov/Drugs/DrugSafety/ucm455386.htm>
53. Robert P, Lehericy S, Grand S, et al. T1-Weighted Hypersignal in the Deep Cerebellar Nuclei After Repeated Administrations of Gadolinium-Based Contrast Agents in Healthy Rats: Difference Between Linear and Macrocyclic Agents. *Invest Radiol* 2015;50:473-80.
54. Wheaton AJ, Miyazaki M. Non-contrast enhanced MR angiography: Physical principles. *J Magn Reson Imaging* 2012;36:286-304.
55. Laub GA. Time-of-flight method of MR angiography.

- Magn Reson Imaging Clin N Am 1995;3:391-8.
56. Wieban O. Cardiovascular Imaging E-Book. Elsevier Health Sciences; 2010.
 57. Krishnam MS, Tomasian A, Malik S, et al. Image quality and diagnostic accuracy of unenhanced SSFP MR angiography compared with conventional contrast-enhanced MR angiography for the assessment of thoracic aortic diseases. *Eur Radiol* 2010;20:1311-20.
 58. Wansapura J, Fleck R, Crotty E, et al. Frequency scouting for cardiac imaging with SSFP at 3 Tesla. *Pediatr Radiol* 2006;36:1082-5.
 59. Wedeen VJ, Rosen BR, Chesler D, et al. MR velocity imaging by phase display. *J Comput Assist Tomogr* 1985;9:530-6.
 60. Joseph P, Tawakol A. Imaging atherosclerosis with positron emission tomography. *Eur Heart J* 2016;37:2974-80.
 61. Rudd JHF, Myers KS, Bansilal S, et al. 18Fluorodeoxyglucose positron emission tomography imaging of atherosclerotic plaque inflammation is highly reproducible. *J Am Coll Cardiol* 2007;50:892-6.
 62. O'Connor S, Andrew P, Batt M, et al. A systematic review and meta-analysis of treatments for aortic graft infection. *J Vasc Surg* 2006;44:38-45.
 63. Legout L, D'Elia PV, Sarraz-Bournet B, et al. Diagnosis and management of prosthetic vascular graft infections. *Med Mal Infect* 2012;42:102-9.
 64. Keidar Z, Nitecki S. FDG-PET in Prosthetic Graft Infections. *Semin Nucl Med* 2013;43:396-402.
 65. Bruggink JL, Glaudemans AW, Saleem BR, et al. Accuracy of FDG-PET-CT in the Diagnostic Work-up of Vascular Prosthetic Graft Infection. *Eur J Vasc Endovasc Surg* 2010;40:348-54.
 66. Keidar Z, Engel A, Hoffman A, et al. Prosthetic vascular graft infection: the role of 18F-FDG PET/CT. *J Nucl Med* 2007;48:1230-6.
 67. Amraoui S, Tlili G, Sohal M, et al. Early prosthetic aortic valve infection identified with the use of positron emission tomography in a patient with lead endocarditis. *J Nucl Cardiol* 2016;23:1504-7.
 68. Swart LE, Scholtens AM, Liesting C, et al. Serial 18F-fluorodeoxyglucose positron emission tomography/CT angiography in transcatheter-implanted aortic valve endocarditis. *Eur Heart J* 2016;37:3059.
 69. Pipitone N, Versari A, Salvarani C. Role of imaging studies in the diagnosis and follow-up of large-vessel vasculitis: an update. *Rheumatology* 2008;47:403-8.
 70. de Boysson H, Liozon E, Lambert M, et al. 18F-fluorodeoxyglucose positron emission tomography and the risk of subsequent aortic complications in giant-cell arteritis: A multicenter cohort of 130 patients. *Medicine (Baltimore)* 2016;95:e3851.
 71. Soussan M, Nicolas P, Schramm C, et al. Management of large-vessel vasculitis with FDG-PET: a systematic literature review and meta-analysis. *Medicine (Baltimore)* 2015;94:e622.
 72. Mavrogeni S, Markousis-Mavrogenis G, Kolovou G. IgG4-related cardiovascular disease. The emerging role of cardiovascular imaging. *Eur J Radiol* 2017;86:169-75.
 73. Yabusaki S, Oyama-Manabe N, Manabe O, et al. Characteristics of immunoglobulin G4-related aortitis/periaortitis and periarteritis on fluorodeoxyglucose positron emission tomography/computed tomography co-registered with contrast-enhanced computed tomography. *EJNMMI Res* 2017;7:20.
 74. Kotze CW, Rudd JH, Ganeshan B, et al. CT signal heterogeneity of abdominal aortic aneurysm as a possible predictive biomarker for expansion. *Atherosclerosis* 2014;233:510-7.
 75. Nchimi A, Cheramy-Bien JP, Gasser TC, et al. Multifactorial relationship between 18F-fluoro-deoxyglucose positron emission tomography signaling and biomechanical properties in unruptured aortic aneurysms. *Circ Cardiovasc Imaging* 2014;7:82-91.
 76. Morel O, Mandry D, Micard E, et al. Evidence of cyclic changes in the metabolism of abdominal aortic aneurysms during growth phases: 18F-FDG PET sequential observational study. *J Nucl Med* 2015;56:1030-5.
 77. Sakalihan N, Van Damme H, Gomez P, et al. Positron emission tomography (PET) evaluation of abdominal aortic aneurysm (AAA). *Eur J Vasc Endovasc Surg* 2002;23:431-6.
 78. Jalalzadeh H, Indrakusuma R, Planken RN, et al. Inflammation as a predictor of abdominal aortic aneurysm growth and rupture: a systematic review of imaging biomarkers. *Eur J Vasc Endovasc Surg* 2016;52:333-42.
 79. Tatsumi M, Cohade C, Nakamoto Y, et al. Fluorodeoxyglucose Uptake in the Aortic Wall at PET/CT: possible finding for active atherosclerosis. *Radiology* 2003;229:831-7.
 80. Rudd JH, Warburton EA, Fryer TD, et al. Imaging atherosclerotic plaque inflammation with [18F]-fluorodeoxyglucose positron emission tomography. *Circulation* 2002;105:2708-11.
 81. Buscombe JR. Exploring the nature of atheroma and cardiovascular inflammation in vivo using positron emission tomography (PET). *Br J Radiol*

- 2015;88:20140648.
82. Pipitone N, Salvarani C, Versari A. Do we need FDG-PET/CT to assess atherosclerosis? *Eur J Nucl Med Mol Imaging* 2017;44:247-8.
 83. Tarkin JM, Joshi FR, Rudd JH. PET imaging of inflammation in atherosclerosis. *Nat Rev Cardiol* 2014;11:443-57.
 84. Moreno PR, Falk E, Palacios IF, et al. Macrophage infiltration in acute coronary syndromes. Implications for plaque rupture. *Circulation* 1994;90:775-8.
 85. Libby P, Ridker PM, Maseri A. Inflammation and Atherosclerosis. *Circulation* 2002;105:1135-43.
 86. Figueroa AL, Abdelbaky A, Truong QA, et al. Measurement of arterial activity on routine FDG PET/CT images improves prediction of risk of future CV events. *JACC Cardiovasc Imaging* 2013;6:1250-9.
 87. Tawakol A, Fayad ZA, Mogg R, et al. Intensification of statin therapy results in a rapid reduction in atherosclerotic inflammation. *J Am Coll Cardiol* 2013;62:909-17.
 88. Silvera SS, Aidi HE, Rudd JH, et al. Multimodality imaging of atherosclerotic plaque activity and composition using FDG-PET/CT and MRI in carotid and femoral arteries. *Atherosclerosis* 2009;207:139-43.
 89. Fleg JL, Stone GW, Fayad ZA, et al. Detection of high-risk atherosclerotic plaque. *JACC Cardiovasc Imaging* 2012;5:941-55.
 90. The American College of Radiology, with more than 30,000 members, is the principal organization of radiologists, radiation onc - 102C4741C2A44691939F0E E3258E0BD2.pdf [Internet]. [cited 2017 Jun 16]. Available online: <https://www.acr.org/~media/102C4741C2A44691939F0EE3258E0BD2.pdf>
 91. Mell MW, Garg T, Baker LC. Under-utilization of routine ultrasound surveillance after endovascular aortic aneurysm repair. *Ann Vasc Surg* 2017;44:54-8.
 92. Guo Q, Zhao J, Huang B, et al. A systematic review of ultrasound or magnetic resonance imaging compared with computed tomography for endoleak detection and aneurysm diameter measurement after endovascular aneurysm repair. *J Endovasc Ther* 2016;23:936-43.
 93. Bredahl KK, Taudorf M, Lönn L, et al. Contrast enhanced ultrasound can replace computed tomography angiography for surveillance after endovascular aortic aneurysm repair. *Eur J Vasc Endovasc Surg* 2016;52:729-34.
 94. Schaeffer JS, Shakhnovich I, Sieck KN, et al. Duplex ultrasound surveillance after uncomplicated endovascular abdominal aortic aneurysm repair. *Vasc Endovascular Surg* 2017;51:295-300.
 95. Rübenthaler J, Reiser M, Cantisani V, et al. The value of contrast-enhanced ultrasound (CEUS) using a high-end ultrasound system in the characterization of endoleaks after endovascular aortic repair (EVAR). *Clin Hemorheol Microcirc* 2017;66:283-92.
 96. Partovi S, Kaspar M, Aschwanden M, et al. Contrast-enhanced ultrasound after endovascular aortic repair—current status and future perspectives. *Cardiovasc Diagn Ther* 2015;5:454.
 97. Lowe C, Abbas A, Rogers S, et al. Three-dimensional contrast-enhanced ultrasound improves endoleak detection and classification after endovascular aneurysm repair. *J Vasc Surg* 2017;65:1453-9.
 98. Mazzei MA, Guerrini S, Mazzei FG, et al. Follow-up of endovascular aortic aneurysm repair: Preliminary validation of digital tomosynthesis and contrast enhanced ultrasound in detection of medium- to long-term complications. *World J Radiol* 2016;8:530.

Cite this article as: Baliyan V, Verdini D, Meyersohn NM. Noninvasive aortic imaging. *Cardiovasc Diagn Ther* 2018;8(Suppl 1):S3-S18. doi: 10.21037/cdt.2018.02.01